Journal of Hydrology 512 (2014) 168–176

Contents lists available at ScienceDirect

Journal of Hydrology

journal homepage: www.elsevier.com/locate/jhydrol

Rainfall kinetic energy controlling erosion processes and sediment sorting on steep hillslopes: A case study of clay loam soil from the Loess Plateau, China

L. Wang [a,b], Z.H. Shi [a,c,*], J. Wang [c], N.F. Fang [a], G.L. Wu [a], H.Y. Zhang [a,b]

[a] State Key Laboratory of Soil Erosion and Dryland Farming on the Loess Plateau, Institute of Soil and Water Conservation, CAS and MWR, Yangling, Shaanxi Province 712100, PR China
[b] University of Chinese Academy of Sciences, Beijing 100049, PR China
[c] College of Resources and Environment, Huazhong Agricultural University, Wuhan 430070, PR China

ARTICLE INFO

Article history:
Received 3 December 2013
Received in revised form 7 February 2014
Accepted 27 February 2014
Available online 12 March 2014
This manuscript was handled by Geoff Syme, Editor-in-Chief

Keywords:
Rainfall kinetic energy
Sediment size
Transport mechanisms

SUMMARY

Rainfall kinetic energy (KE) can break down aggregates in the soil surface. A better understanding of sediment sorting associated with various KEs is essential for the development and verification of soil erosion models. A clay loam soil was used in the experiments. Six KEs were obtained (76, 90, 105, 160, 270, and 518 J m^{-2} h^{-1}) by covering wire screens located above the soil surface with different apertures to change the size of raindrops falling on the soil surface, while maintaining the same rainfall intensity (90 ± 3.5 mm h^{-1}). For each rainfall simulation, runoff and sediment were collected at 3-min intervals to investigate the temporal variation of the sediment particle size distribution (PSD). Comparison of the sediment effective PSD (undispersed) and ultimate PSD (dispersed) was used to investigate the detachment and transport mechanisms involved in sediment mobilization. The effective–ultimate ratios of clay-sized particles were less than 1, whereas that of sand-sized particles were greater than 1, suggesting that these particles were transported as aggregates. Under higher KE, the effective–ultimate ratios were much closer to 1, indicating that sediments were more likely transported as primary particles at higher KE owing to an increased severity of aggregate disaggregation for the clay loam soil. The percentage of clay-sized particles and the relative importance of suspension–saltation increased with increasing KE when KE was greater than 105 J m^{-2} h^{-1}, while decreased with increasing KE when KE was less than 105 J m^{-2} h^{-1}. A KE of 105 J m^{-2} h^{-1} appeared to be a threshold level beyond which the disintegration of aggregates was severe and the influence of KE on erosion processes and sediment sorting may change. Results of this study demonstrate the need for considering KE-influenced sediment transport when predicting erosion.

1. Introduction

Soil erosion by water involves the detachment of soil particles by raindrop impacts and the subsequent transportation of particles by overland flow (Pieri et al., 2009; Warrington et al., 2009). The importance of raindrop impact in sediment detachment has been shown in both laboratory and field settings (Martínez-Mena et al., 1999, 2002; Issa et al., 2006; Asadi et al., 2007a; Pieri et al., 2009) and has been incorporated into the most commonly used models for predicting soil loss, e.g., RUSLE (Renard et al., 1991) and WEPP (Nearing et al., 1989). Many previous studies have focused on the effects of rainfall properties, such as the drop size and velocity, drop shape, kinetic energy (KE), and intensity, on erosion processes (Riezebos and Epema, 1985; Jayawardena and Rezaur, 2000; Salles and Poesen, 2000; Martínez-Mena et al., 2002; Wei et al., 2007; Pieri et al., 2009). Rainfall intensity is a contributing factor to the runoff and sediment generation (Martínez-Mena et al., 1999; Wei et al., 2007). However, the role of rainfall intensity is ambiguous when the infiltration capacity of the soil is exceeded during short-duration, high-intensity storms as well as long duration, low-intensity storms, both of which may cause erosion. Energy parameters are now generally accepted as being better predictors of rainfall erosivity over a wide range of conditions (Stocking and Elwell, 1976). Data on the KE load of rainstorms are essential to developing and verifying models of soil detachment by raindrop impact on interrill erosion processes (Jayawardena and Rezaur, 1999). Relating KE to easily measured

* Corresponding author at: College of Resources and Environment, Huazhong Agricultural University, Wuhan 430070, PR China. Tel.: +86 27 87288249; fax: +86 27 80 02171035.
E-mail address: shizhihua70@gmail.com (Z.H. Shi).

http://dx.doi.org/10.1016/j.jhydrol.2014.02.066
0022-1694/

rainfall parameters would be more practical and convenient to estimate the erosiveness of rainstorms.

The KE of raindrops is used to overcome the bonding effects that hold particles in the soil surface and may also be used in the transport of the detached particles away from the site of impact (Kinnell, 2005). When water flow develops on the soil surface, raindrops penetrate through the flow to detach soil particles, and subsequent drop impacts repeatedly lift the particles into the flow, further moving them downstream on each impact (Kinnell, 2005). The transport of sediment includes a process of soil particle-size selectivity, and the particle size distribution (PSD) of eroded sediment may provide basic information regarding erosion processes (Nearing et al., 1989; Hairsine and Rose, 1992a,b). Particle size data are available for numerous soils and sediments, although these are commonly evaluated after the sediment is fully dispersed into its primary particles. Such data are termed the 'ultimate' PSD (Slattery and Burt, 1997), which is generally recognized as an adequate indicator of pollution potential (Meyer et al., 1992). However, sediment leaving an eroding area consists of both soil aggregates and primary particles (sand, silt, and clay) (Mitchell et al., 1983), and such data may be termed as the 'effective' PSD (Martínez-Mena et al., 2002). Numerous studies have demonstrated that the effective PSD may govern the actual behavior of sediment transport (Slattery and Burt, 1997), particularly influencing the predominance of different sediment transport mechanisms, including suspension, saltation, and rolling. In certain cases, the mass fraction of different sediment sizes is distributed bimodally, including the peaks for a finer size class and a larger size class (Asadi et al., 2007a,b). The bimodal distribution of sediment sizes results from two different mechanisms, suspension–saltation and rolling, which predominately act on different classes of sediment size (Asadi et al., 2007b).

Approximately 800 million people worldwide depend directly on steeplands for their sustenance (Drees et al., 2003). We previously studied soil erosion processes and sediment sorting with varying steep slopes (Shi et al., 2012). However, rainfall KE effects on soil erosion processes and sediment sorting that occur under steep slope conditions are not clear. Lands with slopes between 10° and 20° are widely used for cropping in China. Therefore, a slope of 15° was chosen in this study for further investigation into the temporal changes in eroded sediment-size distribution under different rainfall KEs. The specific objectives of this study were as follows: (1) to measure the sediment PSD with and without dispersion treatment to obtain detailed information regarding sediment sorting under various rainfall KEs and (2) to investigate the effect of rainfall KE on sediment transport mechanisms.

2. Materials and methods

2.1. Experimental devices

The experiments were conducted using a rainfall simulator at the State Key Laboratory of Soil Erosion and Dryland Farming on the Loess Plateau. Rainfall intensities were changed by varying the nozzle sizes and water pressure. Tap water (electrical conductivity 0.7 dS m^{-1}) was used in all experiments. The length, width, and depth of the erosion tray were 2.00, 1.00, and 0.35 m, respectively. A metal runoff collector was set at the end of each tray to direct runoff with sediment into a container. The soil used in the experiments was a clay loam soil collected from Yangling in Shaanxi Province, China. The bulk density of the undisturbed soil in the field was between 1.2 and 1.3 g cm^{-3}. Mean weight diameter (MWD) of aggregates of the original soil after wet sieving was 0.06 mm. The effective and ultimate particle size distribution of the original soil was presented by Fig. 1. Some of the important soil

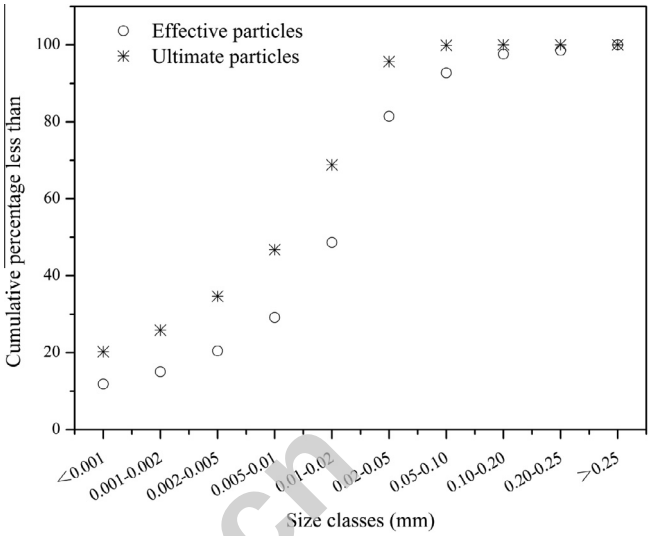

Fig. 1. Effective and ultimate particle size distribution of the original soil used in the study.

chemical properties were determined by Wu et al. (2012) and listed in Table 1.

2.2. Rainfall simulation

The soil was air-dried, and un-decomposed plant residuals were removed after collection from the field. It was then crushed and passed through a 10.0-mm sieve and mixed thoroughly. The soil moisture was measured and kept at ~10% (gravimetric moisture content) to calculate the weight of the soil samples and to fill the trays to a depth of 30 cm. The erosion tray was divided horizontally into three parts (in three 10-cm layers), and the soils were packed in each part separately. Each soil layer was raked lightly before the next layer was packed to diminish the discontinuity between layers. Soils were gently compacted in each layer for diminishing aggregate breakdown and then obtaining a bulk density of ~1.25 g cm^{-3}. A thin sheet of soil was glued onto the walls of the soil tray such that the packed soils were coherent with the walls to prevent ponding of water at the lower end of the erosion trays.

The simulated rainfall intensity was 90 ± 3.5 mm h^{-1}, corresponding to the typical rainfall intensity in sub-humid climate regions of China (Cai et al., 1998). Rainfall KE was varied by covering wire screens located above the soil surface with different apertures to change the size of the raindrops falling on the soil surface while maintaining the same rainfall intensity. Different raindrop sizes were obtained by allowing large raindrops to be intercepted by wire screens with different apertures. The erosion trays were adjusted to a slope of 15° and covered by wire screens placed ~5 cm above the soil surface before being subjected to the rainfall. Raindrop size and velocity were measured after passing the wire screens by a laser precipitation monitor (Thies Clima, Germany), which can directly detect respective raindrop size and velocity passing through its laser beam within 1 min time interval. The

Table 1
Chemical properties of the original soil used in the study.

Soil property	Value	Unit
pH (in H_2O)	8.4	–
Organic matter content	6	g kg^{-1}
Cation exchange capacity (CEC)	17.8	$cmol_c$ kg^{-1}
Exchangeable sodium percentage (ESP)	0.73	%

median volume diameter value of the raindrops (D_{50}) for the intensity of 90 mm h^{-1} applied to the soil surface without covering was 1.61 mm, whereas D_{50} values were 0.73, 0.83, 0.88, 1.31 and 1.43 mm after passing the wire screen with apertures of 0.73, 1.00, 1.41, 2.14, and 5.00 mm, respectively. On the basis of the raindrop size and velocity, KE can be calculated. The KE for the intensity of 90 mm h^{-1} applied to the soil surface without covering was 518 J m^{-2} h^{-1}, whereas the trays covered by wire screens with apertures of 0.73, 1.00, 1.41, 2.14, and 5.00 mm were subjected to KEs of 76, 90, 105, 160, and 270 J m^{-2} h^{-1}, respectively. All treatments had three replications.

2.3. Measurements

2.3.1. Runoff and sediment measurements

The runoff start time was recorded under different KEs, and the water temperature was measured. Runoff with sediment was collected in a bucket at 3-min intervals. Collected samples were weighed, separated from the water and dried in a forced-air oven at 105 °C until a constant mass was achieved. The amount of dried, eroded sediment was weighed to obtain the amount of soil loss and runoff volume. The runoff rate, stream power, sediment concentration, and soil loss rate were calculated. Steam power (ω, W m^{-2}) is the energy of runoff per unit area, some or all of which may be available to remove and transport aggregates from the erosion surface (Teixeira and Misra, 1997). Stream power was calculated as follows:

$$\omega = \rho g S q, \quad (1)$$

where ρ is the density of water (assumed to have a constant value of 1000 kg m^{-3} at 25 °C), g is the gravitational acceleration (9.8 m s^{-2}), S is the sine of the erosion surface slope, and q is the unit width flow rate of erosion surface (m^2 s^{-1}).

2.3.2. Measurement of particle size distribution

Runoff with sediment was also collected in a beaker at 3-min intervals during rainfall to measure the sediment-size distribution. The sampling duration was 2–3 s, which was adapted to the requirements of the size-distribution measurement. The collected samples were immediately transported to the laboratory to analyze the effective PSD using a Malvern Mastersizer 2000 laser diffraction device (Malvern Instruments Ltd., UK). After determining the effective PSD of the sediment, subsamples were treated with hydrogen peroxide to remove organic matter, dispersed in sodium hexametaphosphate, and then subjected to ultrasonic dispersion to obtain the ultimate PSD of the sediment using the Malvern Mastersizer 2000 laser diffraction device. The sediment effective PSD data were used to investigate the detachment and transport mechanisms involved in sediment mobilization, and a comparison of the sediment effective PSD with the sediment ultimate PSD provided a measure of the particle-size selectivity during erosion processes. The effective and ultimate PSD of the original soil were measured using the previously mentioned procedure used to measure sediment size.

2.4. Data analysis

The effective PSD data of the original soil were subdivided into 10 size classes, each having an equal mass fraction. The fraction of each size class in the outflow sediment at different times during each experiment was then obtained using the subdivision of equal classes obtained for the original soil. Using the same size class boundaries obtained from subdivision of the original soil into equal mass classes, the fraction of eroded materials in the outflow from the plot was determined for each size class (Asadi et al., 2007a). The outflow sediment concentration in each size class of eroded materials was then obtained by multiplying the total sediment concentration by the fraction of each size class. The detailed procedure was reported in our previous study (Shi et al., 2012).

3. Results

3.1. Runoff and soil loss

Table 2 shows the results from all the rainfall simulation experiments under different rainfall KEs. Compared with the KE applied to the bare soil surface (KE = 518 J m^{-2} h^{-1}), the KE was reduced by approximately 48%, 69%, 80%, 83%, and 85% when soils were covered by wire screens of apertures of 5.00, 2.14, 1.41, 1.00, and 0.73 mm, respectively. The time to runoff commencement (T_q) decreased significantly with increasing KE ($p < 0.01$). A higher KE leads to a greater runoff rate (q_r) and stream power (ω), which may directly affect the shear force and carrying capacity of the runoff, such that the sediment concentration (C_s) and soil loss rate (S_r) are correspondingly variable for different KE ($p < 0.01$). The sediment concentration was reduced by 65.8%, 68.3%, 70.7%, 75.6% and 80.5%, respectively, when the KE was reduced by 48%, 69%, 80%, 83%, and 85%, respectively. The soil loss rate was reduced by 72.1%, 72.7%, 73.3%, 81.5% and 85.4%, respectively, when the KE was reduced by 48%, 69%, 80%, 83%, and 85%, respectively. Fig. 2 illustrates the temporal variation of the runoff rate, soil loss rate, and sediment concentration under different KE values. Changes in the runoff rate with time for different KEs showed a similar and clear pattern: the runoff rate increased quickly during the initial minutes and then approached a constant (Fig. 2a). The soil loss rate at various KEs showed two different patterns: the soil loss rate initially decreased rapidly when KE $\geqslant$ 160 J m^{-2} h^{-1} and increased rapidly when KE < 160 J m^{-2} h^{-1} (Fig. 2b). The sediment concentration decreased over time and then became relatively constant when KE $\leqslant$ 270 J m^{-2} h^{-1} (Fig. 2c). Conversely, the sediment concentration and soil loss rate increased slightly after a sharp decrease in the KE of 518 J m^{-2} h^{-1}.

Table 2
Erosional responses of different rainfall kinetic energies.*

KE (J m^{-2} h^{-1})	T_q (Min)	q_r (L m^{-2} min^{-1})	ω (W m^{-2})	C_s (kg L^{-1})	S_r (g m^{-2} min^{-1})	$D_{0.5e}$ (μm)	$D_{0.5u}$ (μm)
76	4.77a	0.743c	0.063c	0.008c	5.11b	23.12b	12.85abc
90	4.24ab	0.781bc	0.066bc	0.010c	6.47b	25.59b	12.78ad
105	4.02b	0.782bc	0.066bc	0.012bc	9.34b	31.05a	13.06ac
160	3.94b	0.815b	0.069b	0.013bc	9.56b	23.85b	12.50bd
270	3.79b	0.817b	0.069b	0.014b	9.74b	23.74b	12.12e
518	3.19c	0.891a	0.075a	0.041a	34.96a	15.56c	12.47de

Values in a column with the same letter(s) are not significantly different at $p < 0.05$.
* KE: rainfall kinetic energy; T_q: time to start runoff; q_r: runoff rate; ω: stream power; C_s: sediment concentration; S_r: soil loss rate; $D_{0.5e}$: median diameter of effective particles; $D_{0.5u}$: median diameter of ultimate particles.

3.2. Rainfall kinetic energy affects effective sediment size

The differences in the median diameters of the effective eroded particles under different KEs were significant ($p < 0.01$) (Table 2). The sediment sizes were classified as clay-size (<0.002 mm), fine silt-size (0.002–0.02 mm), coarse silt-size (0.02–0.05 mm), fine sand-size (0.05–0.25 mm), and coarse sand-size (>0.25 mm). Fig. 3 shows the average percentage of these five sediment-size classes under different KEs, which suggests that a KE of approximately 105 J m^{-2} h^{-1} is a likely threshold level. The average percentage of clay- and silt-sized sediment particles increased with increasing KE (>105 J m^{-2} h^{-1}), whereas the percentage of sand-sized sediment decreased. However, the average percentage of these five sediment-size classes shows an opposite trend when KE < 105 J m^{-2} h^{-1}, with the average percentage of clay- and silt-sized sediment particles decreasing, and the percentage of sand-sized sediment increasing, with increasing KE. The coarse sand-sized aggregates were almost completely destroyed (the percentage of coarse sand was 0.9%) when KE = 518 J m^{-2} h^{-1}. Fig. 4 shows the temporal variations of the effective sediment-particle percentages for different KEs. The sediment for different KEs was mainly composed of silt-sized particles (0.002–0.05 mm) at any given moment during the rainfall and accounted for approximately 50–70% of the sediment load (Fig. 4). The percentage of sand-sized particles decreased with time in all experiments. The percentage of the five sediment size classes showed small fluctuations when KE = 518 J m^{-2} h^{-1}, whereas the percentage of the five sediment classes showed relatively large fluctuations when the KE was relatively low.

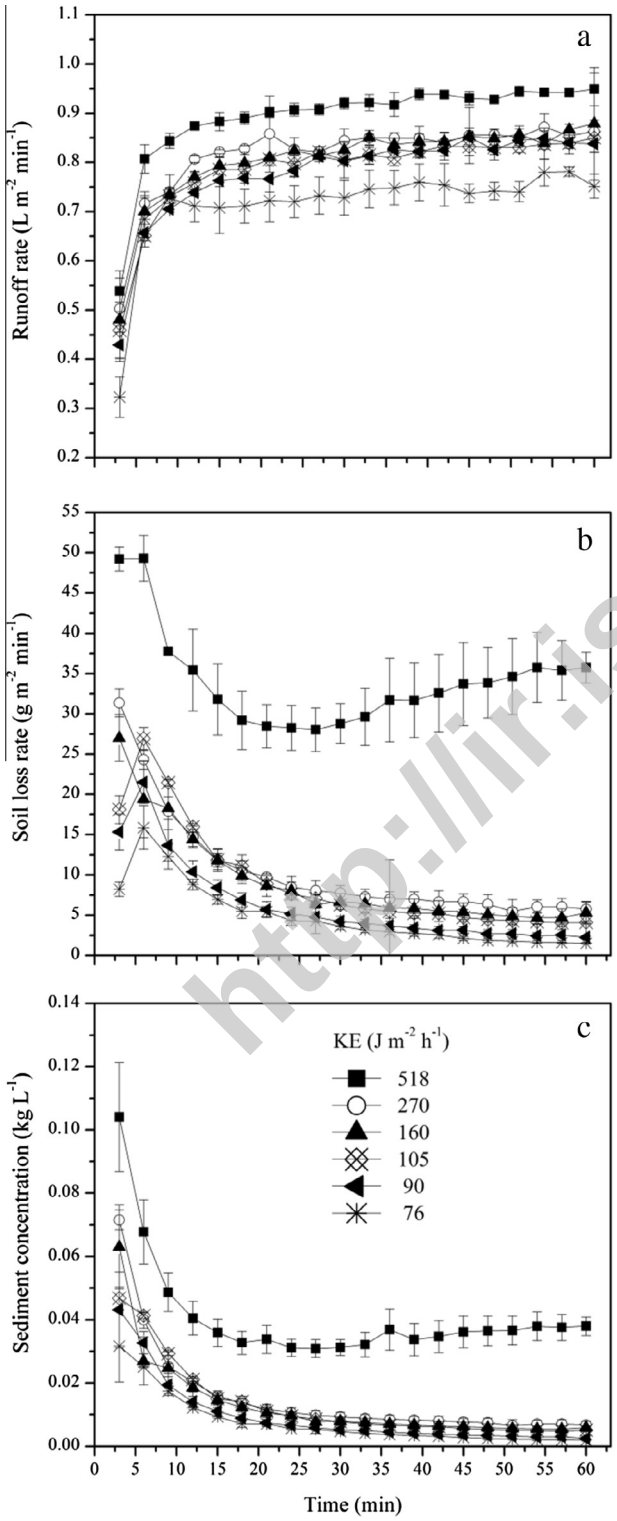

Fig. 2. Temporal variation in the runoff rate, soil loss rate, and sediment concentration under different rainfall kinetic energies (KEs): (a) runoff rate, (b) soil loss rate, and (c) sediment concentration.

3.3. Comparison of effective and ultimate sediment size distribution

The median diameter of the effective particles in all experiments was considerably greater than that of the ultimate particles (Table 2). The relative proportion of the effective and ultimate particle sizes may be considered as an indicator of how the different fractions are eroded and transported by the flow (Martínez-Mena et al., 2002). An effective–ultimate ratio of 1 indicates that the sediment is transported as primary particles, whereas a ratio of greater or lower than 1 indicates that the sediment is transported as aggregates (Martínez-Mena et al., 2002). Fig. 5 represents the temporal variation in the effective–ultimate ratios for clay-, fine silt-, coarse silt-, and sand-sized particles. The effective–ultimate ratios for clay-sized particles were all less than 1 for all stages of the erosion process under different KEs and increased with increasing KE when KE > 105 J m^{-2} h^{-1} (Fig. 5a). The effective–ultimate ratios of the fine silt-sized particles were close to 1 after ~25 min from the beginning of rainfall when KE = 518 J m^{-2} h^{-1}, whereas the ratios were less than 1 when KE < 518 J m^{-2} h^{-1} (Fig. 5b). For nearly the entire experiment, the effective–ultimate ratios of coarse silt-sized particles fluctuated at an approximate value of 1 (Fig. 5c). The effective–ultimate ratios for sand-sized particles were always

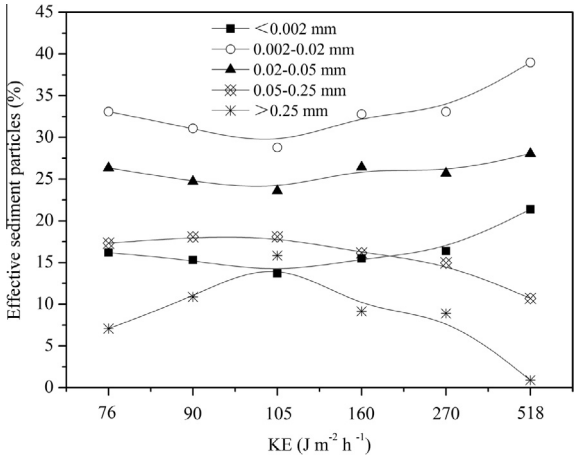

Fig. 3. Changes in the average percentage of effective sediment particles under different rainfall kinetic energies (KEs).

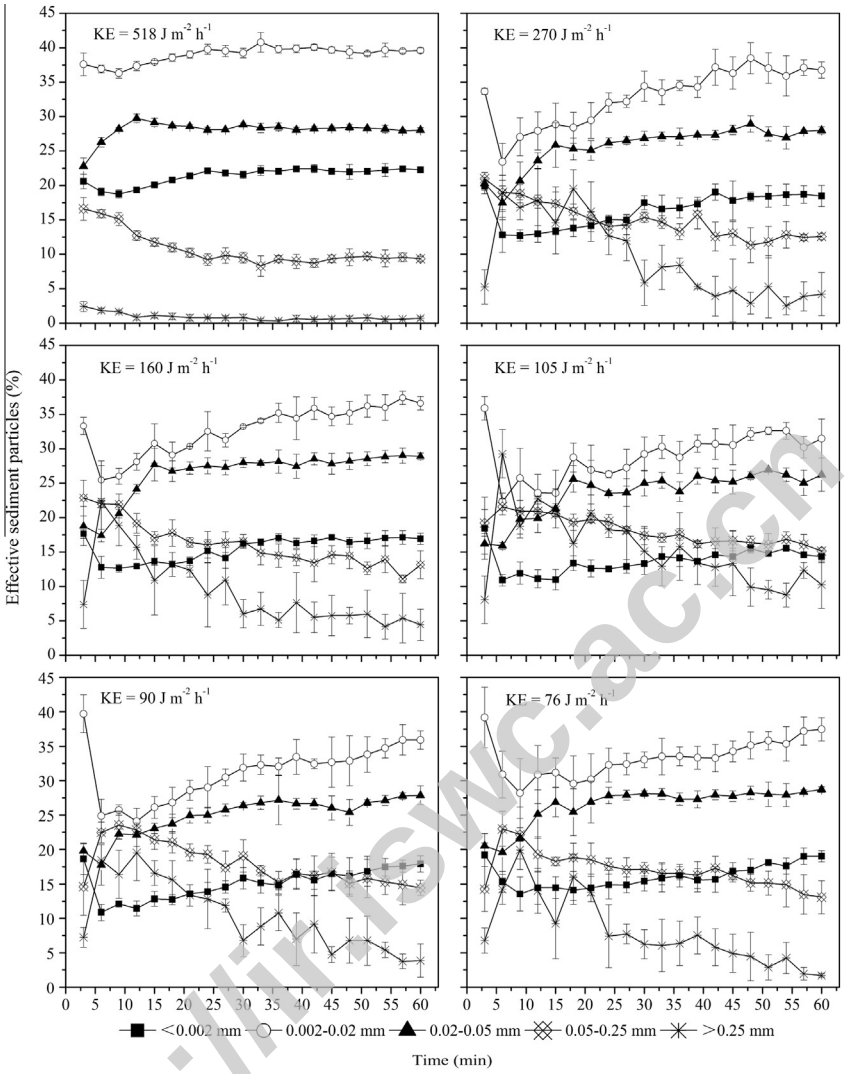

Fig. 4. Temporal variation in the percentage of effective sediment particles under different rainfall kinetic energies (KEs).

greater than 1 (Fig. 5d). In addition, the effective–ultimate ratios of the clay- and fine silt-sized particles exhibited an increasing trend with time, whereas that of the sand-sized particles exhibited a decreasing trend (Fig. 5).

3.4. Sediment transport mechanisms

Fig. 6 presents the percentage of the 10 size classes in the outflow at three different sampling times under different KEs. The original soil consisted of 10 equal mass fractions in each size class, indicated in Fig. 6 by a uniform original fraction of 10%. Eroded sediment fractions greater than 10% can be said to be preferentially transported. Fig. 6 shows a bimodal distribution of particle size classes with peaks for a finer size class of <0.016 mm and a larger size class of >0.105 mm when KE $\leqslant$ 270 J m^{-2} h^{-1}. In contrast, fractions in a size class tend to decrease gradually with increasing size for the three sampling times when KE = 518 J m^{-2} h^{-1} (Fig. 6). Sediment transport can be divided into suspended, saltating, and contact (rolling) loads (Moss et al., 1979), and a bimodal distribution of sediment size may result from two different transport mechanisms, rolling and suspension–saltation, each acting predominantly on particles of different size classes (Asadi et al., 2007b). Size classes with minimum transport rates provide a border between suspension–saltation and bed-load transport (Asadi et al., 2011). The bed load becomes a considerable sediment transport mechanism beyond the size class with a minimum transport rate. The size classes with the lowest sediment transport rate (LST) slightly increase with time: LST between 0.032–0.105 mm at 3–6 min and LST between 0.059–0.105 mm at 24–27 min and 54–57 min (Fig. 6). Soil particles of different size classes were all transported by suspension–saltation or bed load in the experiment, so the relative importance of suspension–saltation means the percentage of soil particles transported by suspension–saltation. Table 3 shows the relative importance of each transport mechanism at three sampling times under different KEs. Greater than 50% of soil particles were transported by suspension–saltation, with an increase in the relative importance of suspension–saltation with time under different KEs. In addition, the relative importance of suspension–saltation increased with increasing KE when KE > 105 J m^{-2} h^{-1} and decreased with increasing KE when KE < 105 J m^{-2} h^{-1}. The relative importance of bed-load transport under different KEs showed an opposite trend.

4. Discussion

The median diameter of the effective sediment particles in all experiments was considerably larger than that of the ultimate sediment particles (Table 2). This result indicates that sediment

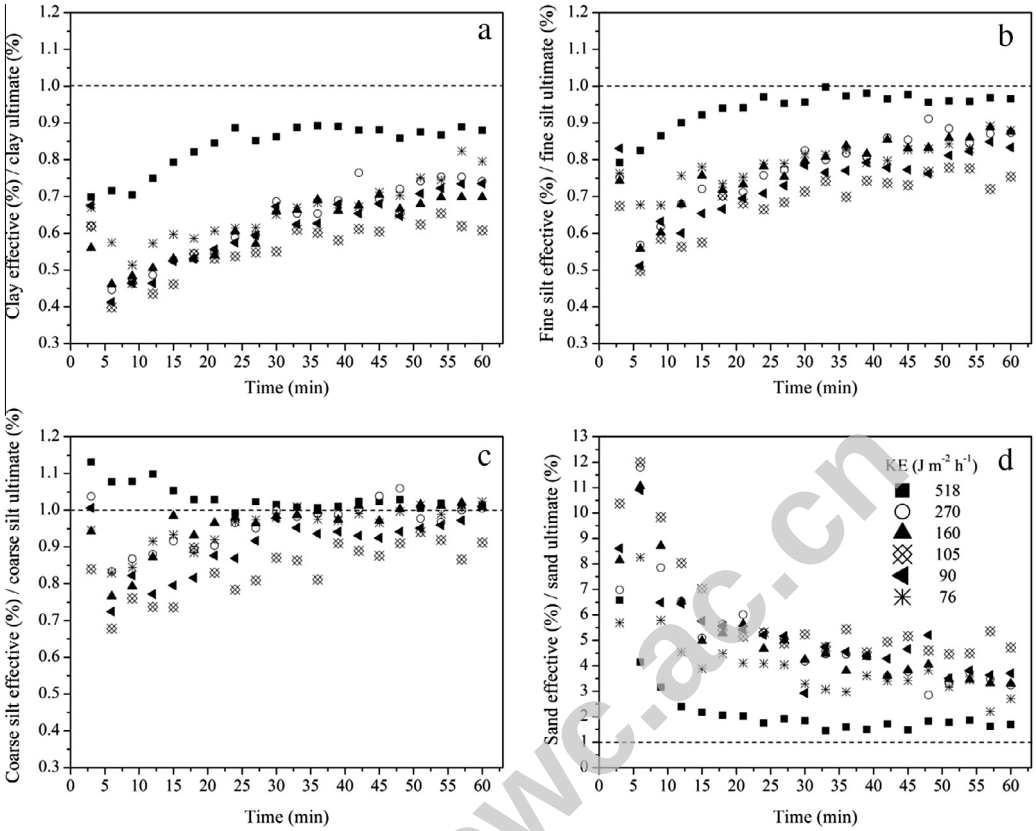

Fig. 5. Comparison of the effective–ultimate ratios in the clay, fine silt, coarse silt, and sand fractions under different rainfall kinetic energies (KEs) (note the different scale on the *y* axis for sand particles).

in the runoff included a substantial proportion of aggregates (Slattery and Burt, 1997; Martínez-Mena et al., 1999, 2002; Shi et al., 2013) and emphasizes the importance of studying the effective sediment (as well as the ultimate sediment) because the use of primary particle size data in transport mechanisms may provide erroneous results owing to substantial quantities of clay that are often transported in aggregate form (Beuselinck et al., 2000). Clay-, fine silt-, and sand-sized sediments are preferentially transported as aggregates compared with coarse silt-sized sediments under a lower KE (Fig. 5). A higher KE leads to a larger amount of sediment transported as primary particles, which is reflected by effective–ultimate ratios much closer to 1 at higher KE because of more severe disintegration of aggregates at higher KE. Aggregate breakdown results in an enrichment of fine-sized particles, especially clay-sized particles, which is particularly important in agricultural areas because most of the nutrients and contaminants are bound by these particles.

Many studies have found that the breakdown of aggregates by KE is only dominant during the initial minutes of a storm (Martínez-Mena et al., 2002; Kinnell, 2005). Fine-sized particles released by KE may move down the soil profile to 0.1–0.5 mm depth and accumulate, clogging conducting pores (Agassi et al., 1981) and generating overland flows. When overland flows are initiated, raindrops penetrate through the flow to detach soil particles, and subsequent drop impacts lift the particles into the flow, moving the particles downstream on each occasion (Kinnell, 2005). Raindrop impact may increase the turbulence of the flowing surface water, which in turn enhances the erosive power of overland flow (Bradford et al., 1987). The disintegration of aggregates by KE may almost vanish when the flowing surface water is deep enough to absorb all raindrop energy (Ferreira and Singer, 1985; Asadi et al., 2007a). The effective–ultimate ratios of the four different sized particles progressively approached a value of 1 with time (Fig. 5), suggesting that an increasing amount of sediment is transported as primary particles with time and indicating that aggregate breakdown may also be caused by flow mechanisms (Gabriels and Moldenhauer, 1978). The percentage of sand-sized sediment particles (>0.05 mm) decreased with time in all simulation rainfall experiments under different KEs (Fig. 4), demonstrating the breakdown of aggregates caused by raindrop impact and flow mechanics. However, Martínez-Mena et al. (2002) and Shi et al. (2012) found that the percentage of coarse particles increased with time due to time-dependent increases in the runoff carrying capacity and the development of a soil crust that impeded the breakdown of aggregates (Le Bissonnais, 1996; Bajracharya and Lal, 1998). Different results in this experiment show that aggregate breakdown by KE and/or flow mechanics is more significant than in previous studies, which is likely because of the different soil types and erosive forces.

Clay-sized particles are commonly associated with aggregation by rearrangement and flocculation (Bronick and Lal, 2005). When rainfall energy is high enough to destroy soil aggregates, clays become available for transport (Durnford and King, 1993). The content of clay-sized sediment in runoff provides an indication of the forces that acted on the aggregates during detachment and transport by the erosive agent (Loch and Donnollan, 1983). Brodowski (2013) reported that a threshold level of KE exists beyond which the KE may detach and eject soil particles and below which the KE may not cause erosion. This result might explain why the median diameter of the effective particles did not continuously increase with decreasing KE when KE < 105 J m^{-2} h^{-1} (Table 2). A KE of approximately 105 J m^{-2} h^{-1} may be a threshold level in this experiment, below which the disintegration of aggregates by KE may be not severe. Detached soil particles travel a limited distance

after each raindrop impact before runoff initiation (Kinnell, 2005), whereas the overland flow plays a major role in moving particles out of slopes from the site of detachment. Assuming that a low KE has little effect on aggregate breakdown but enhances the erosive power of overland flow by increasing its turbulence (Bradford et al., 1987), a higher KE may lead to a greater runoff carrying capacity, and the sediment may contain more relatively large particles, which would decrease the percentage of clay-sized particles. Runoff carrying capacity is small because of the high soil infiltration in the initial minutes of rainfall, leading to declining clay-sized sediment percentages with time as a result of an abundance of transportable fine particles originally contained in soil and released by raindrop impact. After a short duration of decline, clay-sized sediment percentages continuously increase with time, indicating that flow mechanisms participate in the breakdown of aggregates, which was also reflected by Fig. 5 and consistent with Gabriels and Moldenhauer (1978).

Raindrop impact and runoff properties may influence the amount of readily transportable sediments and their transported forms as either a primary particle and/or aggregate, which may correspondingly affect the sediment transport mechanism. Higher KE may lead to more severe aggregate breakdown and enhance the fractions of finer-sized sediments with smaller weight and settling velocity (Hairsine and Rose, 1992a,b), which are more likely transported by suspension–saltation compared with larger-sized sediments. Fig. 6 suggests that suspension–saltation transport is responsible for the first peak of the finer class, and bed-load transport is responsible for the second peak of the coarser class. The upper size limit of particles transported by suspension–saltation slightly increases with time (Fig. 6), which is most likely the result of greater runoff carrying capacity causing coarser particles to be transported by suspension–saltation, which is consistent with Asadi et al. (2011).

The relative importance of suspension–saltation increases with increasing KE (>105 J m^{-2} h^{-1}) (Table 3) because sediments contain

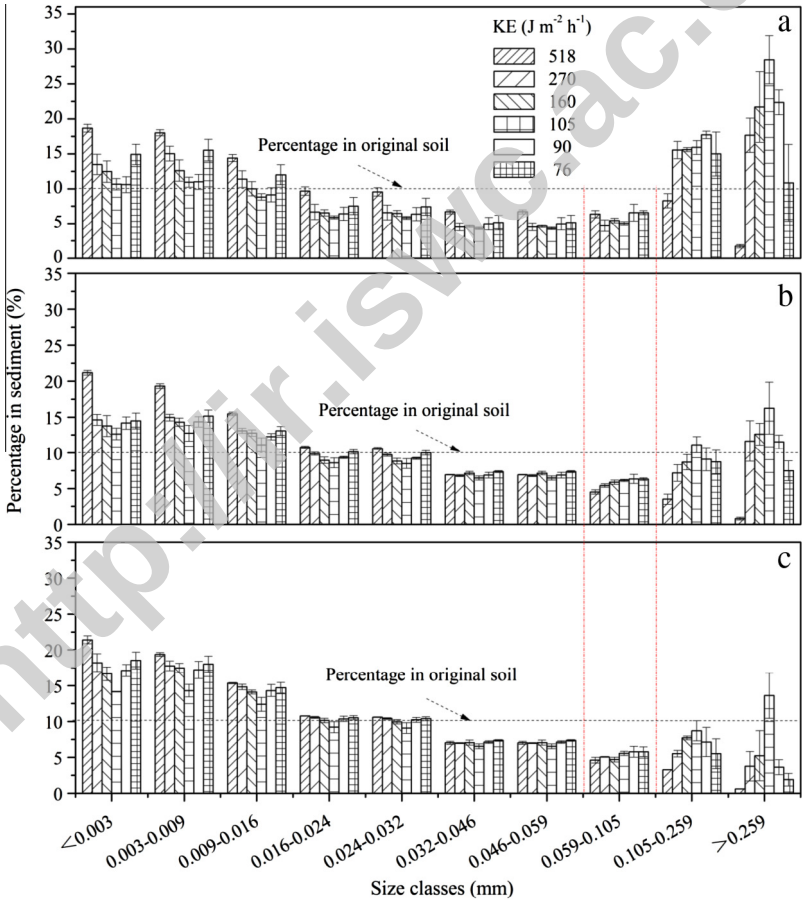

Fig. 6. Percentage of the 10 size classes in outflow sediment for three sampling times: (a) 3–6 min, (b) 24–27 min, and (c) 54–57 min.

Table 3
Relative importance (%) of suspension–saltation and bed-load transport in sediment.

KE	Suspension–saltation			Bed-load transport		
J m^{-2} h^{-1}	3–6 min	24–27 min	54–57 min	3–6 min	24–27 min	54–57 min
76	67.62	77.49	86.84	32.37	22.51	13.16
90	53.37	73.03	83.46	46.63	26.97	16.54
105	50.66	66.51	72.14	49.34	33.49	27.86
160	57.26	74.85	85.28	42.74	25.15	14.62
270	58.13	75.77	85.67	41.87	24.23	14.33
518	83.66	91.17	91.50	16.34	8.83	8.50

larger fractions of fine particles under higher KE. However, the relative importance of suspension–saltation does not continuously increase with increasing KE (<105 J m^{-2} h^{-1}) (Table 3), indicating that KE is not the only factor determining the predominance of the two transport mechanisms, and a KE of approximately 105 J m^{-2} h^{-1} is a likely threshold level that influences the clay-sized sediment percentage and transport mechanisms. As mentioned above, flow mechanisms participate in aggregate breakdown as well as KE. The relationship between the relative importance of suspension–saltation and stream power was investigated by Asadi et al. (2011), who showed that the relative importance of suspension–saltation may reduce significantly with increasing stream power. The relative importance of suspension–saltation increases with time in this experiment (Table 3), as well as the increasing instantaneous stream power under different KEs. This difference occurred most likely because Asadi et al. (2011) did not consider aggregate breakdown during the erosion process. Fine particles transported by suspension–saltation would be supplemented by aggregate breakdown by KE and stream power. Higher stream power leads to larger upper size limit of particles transported by suspension–saltation, which may also enhance the relative importance of suspension–saltation. However, if aggregate breakdown is not considered, the relative importance of suspension–saltation is reduced even when higher stream power increases the upper size limit of particles transported by suspension–saltation, because of the exhaustion of fine particles that are more readily transported by suspension–saltation. KE is positively related with the relative importance of suspension–saltation when KE > 105 J m^{-2} h^{-1} and negatively related with the relative importance of suspension–saltation when KE < 105 J m^{-2} h^{-1} (Table 3), most likely because aggregates can be destroyed by high KE, leading to the release of fine particles that are transported by suspension–saltation. Low KE affects the relative importance of suspension–saltation by increasing runoff carrying capacity, which may lead to an increase of the coarse particle fragment in sediment that is more likely transported by bed-load transport than by suspension–saltation. The results of this experiment emphasize the importance of considering KE when investigating sediment transport mechanisms. Considering the range of stream power is narrow in the experiment, assumptions about the relationship between instantaneous stream power and sediment transport mechanisms may be controversy, so further research is needed to investigate the relationship among rainfall energy, flow energy and sediment transport mechanisms.

The rate of soil loss increased rapidly with increasing runoff rates during the initial stage of erosion when KE $\leqslant$ 105 J m^{-2} h^{-1} (Fig. 2b), owing to the relatively small carrying capacity of runoff that accompanies an abundance of transportable fine particles. However, the increased runoff rate did not increase the rate of soil loss during the initial stage of erosion when KE > 105 J m^{-2} h^{-1} (Fig. 2b), indicating that the runoff may carry more soil particles than the transportable particles which were original contained in the soil and/or released by raindrop impact. With the increasing carrying capacity of runoff and the progressive exhaustion of transportable fine particles loosened by raindrop impact, the rate of soil loss and sediment concentration both decreased with time when KE $\leqslant$ 270 J m^{-2} h^{-1} (Fig. 2b and c). In contrast, the rate of soil loss and sediment concentration both increased slightly after a sharp decrease when KE = 518 J m^{-2} h^{-1}, which indicates that the highest KE in the experiment was large enough to provide transportable fine particles during the erosion process.

5. Conclusions

Erosion processes and sediment sorting for different KEs (76, 90, 105, 160, 270, and 518 J m^{-2} h^{-1}) were studied on a slope of 15° under simulated rainfall using a clay loam soil. A higher KE resulted in a higher abundance of fine particles due to aggregate breakdown. The effective–ultimate ratios of clay-sized particles were smaller than 1, whereas that of sand-sized particles were larger than 1, suggesting that these particles were transported as aggregates. The effective–ultimate ratios were much closer to 1 under higher KE, indicating that sediments were more likely transported as primary particles at higher KE, owing to a more severe disaggregation of aggregates at higher KE. The percentage of clay-sized particles and the relative importance of suspension–saltation increased with increasing KE when KE was greater than 105 J m^{-2} h^{-1}, while decreased with increasing KE when KE is less than 105 J m^{-2} h^{-1}. A KE of 105 J m^{-2} h^{-1} is a likely threshold level, beyond which the influence of KE on erosion processes and sediment sorting may change. When the KE is greater than 105 J m^{-2} h^{-1}, the disintegration of aggregates by KE may be severe leading to more release of fine-sized particles, which may increase the percentage of the clay-sized particles and the relative importance of suspension–saltation. Low KE (<105 J m^{-2} h^{-1}) has little effect on aggregate breakdown but enhances the erosive power of overland flow by increasing its turbulence (Bradford et al., 1987). Higher KE may lead to greater runoff carrying capacity, and the sediment may contain more relatively large particles, which would decrease the percentage of clay-sized particles. Results of this study emphasize that a consideration of the KE associated with erosion processes and sediment sorting is required for effective erosion prediction.

Acknowledgements

Financial support for this research was provided by the National Natural Science Foundation of China (41271296) and the 'Hundred-talent Project' of the Chinese Academy of Sciences.

References

Agassi, M., Shainberg, I., Morin, J., 1981. Effect of electrolyte concentration and soil sodicity on infiltration rate and crust formation. Soil Sci. Soc. Am. J. 45, 848–851.
Asadi, H., Ghadiri, H., Rose, C.W., Rouhipour, H., 2007a. Interrill soil erosion processes and their interaction on low slopes. Earth Surf. Proc. Land. 32, 711–724.
Asadi, H., Ghadiri, H., Rose, C.W., Yu, B., Hussein, J., 2007b. An investigation of flow-driven soil erosion processes at low streampowers. J. Hydrol. 342, 134–142.
Asadi, H., Moussavi, A., Ghadiri, H., Rose, C.W., 2011. Flow-driven soil erosion processes and the size selectivity of sediment. J. Hydrol. 406, 73–81.
Bajracharya, R.M., Lal, R., 1998. Crusting effects on erosion processes under simulated rainfall on a tropical Alfisol. Hydrol. Process. 12, 1927–1938.
Beuselinck, L., Steegen, A., Govers, G., Nachetergaele, J., Takken, I., Poesen, J., 2000. Characteristics of sediment deposits formed by intense rainfall events in small catchments in the Belgian Loam Belt. Geomorphology 32, 69–82.
Bradford, J.M., Ferris, J.E., Remley, P.A., 1987. Interrill soil erosion processes: I. Effect of surface sealing on infiltration, runoff, and soil splash detachment. Soil Sci. Soc. Am. J. 51, 1566–1571.
Brodowski, R., 2013. Soil detachment caused by divided rain power from raindrop parts splashed downward on a sloping surface. Catena 105, 52–61.
Bronick, C.J., Lal, R., 2005. Soil structure and management: a review. Geoderma 124, 3–22.
Cai, Q.G., Wang, G.P., Chen, Y.Z., 1998. Process of sediment yield in a small watershed of the loess plateau and its modeling. Science Press, Beijing, pp. 92–103 (in Chinese).
Drees, L.R., Wilding, L.P., Owens, P.R., Wu, B., Perotto, H., Sierra, H., 2003. Steepland resources: characteristics, stability and micromorphology. Catena 54, 619–636.
Durnford, D., King, J.P., 1993. Experimental study of processes and particle-size distributions of eroded soil. J. Irrig. Drain. Eng. 119, 383–398.
Ferreira, A.G., Singer, M.J., 1985. Energy-dissipation for water drop impact into shallow pools. Soil Sci. Soc. Am. J. 49, 1537–1542.
Gabriels, D., Moldenhauer, W.C., 1978. Size distribution of eroded material from simulated rainfall: effect over a range of texture. Soil Sci. Soc. Am. J. 42, 954–958.
Hairsine, P.B., Rose, C.W., 1992a. Modeling water erosion due to overland flow using physical principles: 1. Sheet flow. Water Resour. Res. 28, 237–243.
Hairsine, P.B., Rose, C.W., 1992b. Modeling water erosion due to overland flow using physical principles: 2. Rill flow. Water Resour. Res. 28, 245–250.
Issa, M.O., Le Bissonnais, Y., Planchon, O., Favis-Mortlock, D., Silvera, N., Wainwright, J., 2006. Soil detachment and transport on field- and laboratory-scale interrill areas: erosion processes and the size-selectivity of eroded sediment. Earth Surf. Proc. Land. 31, 929–939.

Jayawardena, A.W., Rezaur, R.B., 1999. Evaluation of an interrill soil erosion model using laboratory catchment data. Hydrol. Process. 13, 89–100.
Jayawardena, A.W., Rezaur, R.B., 2000. Drop size distribution and kinetic energy load of rainstorms in Hong Kong. Hydrol. Process. 14, 1069–1082.
Kinnell, P.I.A., 2005. Raindrop-impact-induced erosion processes and prediction: a review. Hydrol. Process. 19, 2815–2844.
Le Bissonnais, Y., 1996. Aggregate stability and assessment of soil crustability and erodibility: I. Theory and methodology. Eur. J. Soil Sci. 47, 425–437.
Loch, R.J., Donnollan, T.E., 1983. Field rainfall simulator studies on two clay soils of the Darling Downs, Queensland. II. Aggregate Breakdown, sediment properties and soil erodibility. Aust. J. Soil Res. 21, 47–58.
Martínez-Mena, M., Alvarez Rogel, J., Albaladejo, J., Castillo, V.M., 1999. Influence of vegetal cover on sediment particle size distribution in natural rainfall conditions in a semiarid environment. Catena 38, 175–190.
Martínez-Mena, M., Castillo, V., Albaladejo, J., 2002. Relations between interrill erosion processes and sediment particle size distribution in a semiarid Mediterranean area of SE of Spain. Geomorphology 45, 261–275.
Meyer, L.D., Line, D.E., Harmon, W.C., 1992. Size characteristics of sediment from agricultural soils. J. Soil Water Conserv. 47, 107–111.
Mitchell, J.K., Mostaghimi, S., Pond, M.C., 1983. Primary particle and aggregate size distribution of eroded soil from sequenced rainfall events. Trans. ASAE 26, 1773–1777.
Moss, A.J., Walker, P.H., Hutka, J., 1979. Raindrop-stimulated transportation in shallow water flows: an experimental study. Sediment Geol. 22, 165–184.
Nearing, M.A., Foster, G.R., Lane, L.J., Finkner, S.C., 1989. A process-based soil erosion model for USDA-Water Erosion Prediction Project technology. Trans. ASAE 32, 1587–1593.
Pieri, L., Bittelli, M., Hanuskova, M., Ventura, F., Vicari, A., Pisa, P.R., 2009. Characteristics of eroded sediments from soil under wheat and maize in the North Italian Apennines. Geoderma 154, 20–29.
Renard, K.G., Foster, G.R., Weesies, G.A., Porter, J.P., 1991. RUSLE: revised universal soil loss equation. J. Soil Water Conserv. 46, 30–33.
Riezebos, H.T., Epema, G.F., 1985. Drop shape and erosivity part II: splash detachment, transport and erosivity indices. Earth Surf. Proc. Land. 10, 69–74.
Salles, C., Poesen, J., 2000. Rain properties controlling soil splash detachment. Hydrol. Process. 14, 271–282.
Shi, Z.H., Fang, N.F., Wu, F.Z., Wang, L., Yue, B.J., Wu, G.L., 2012. Soil erosion processes and sediment sorting associated with transport mechanisms on steep slopes. J. Hydrol. 454–455, 123–130.
Shi, Z.H., Yue, B.J., Wang, L., Fang, N.F., Wang, D., Wu, F.Z., 2013. Effects of mulch cover rate on interrill erosion processes and the size selectivity of eroded sediment on steep slopes. Soil Sci. Soc. Am. J. 77, 257–267.
Slattery, M.C., Burt, T.P., 1997. Particle size characteristics of suspended sediment in hillslope runoff and stream flow. Earth Surf. Proc. Land. 22, 705–719.
Stocking, M.A., Elwell, H.A., 1976. Rainfall erosivity over Rhodesia. Trans. Inst. Br. Geogr. 1, 231–245.
Teixeira, P.C., Misra, R.K., 1997. Erosion and sediment characteristics of cultivated forest soils as affected by the mechanical stability of aggregates. Catena 30, 119–134.
Warrington, D.N., Mamedov, A.I., Bhardwaj, A.K., Levy, G.J., 2009. Primary particle size distribution of eroded material affected by degree of aggregate slaking and seal development. Eur. J. Soil Sci. 60, 84–93.
Wei, W., Chen, L., Fu, B., Huang, Z., Wu, D., Gui, L., 2007. The effect of land uses and rainfall regimes on runoff and soil erosion in the semi-arid loess hilly area, China. J. Hydrol. 335, 247–258.
Wu, F.Z., Shi, Z.H., Fang, N.F., 2012. Temporal variations of clay content in eroded sediment under different rainfall condition (in Chinese), Chinese. J. Environ. Sci. 33, 2497–2502.